Available online at www.sciencedirect.com

SCIENCE DIRECT®

Inorganica Chimica Acta 357 (2004) 3712–3720

Inorganica Chimica Acta

www.elsevier.com/locate/ica

Syntheses and structures of vinyl and aryl derivatives of carbonyl halide iron complexes

Chiara Venturi, Gianfranco Bellachioma, Giuseppe Cardaci *, Alceo Macchioni

Dipartimento di Chimica, Università di Perugia, Via Elce di Sotto 8, I-06123 Perugia, Italy

Received 26 March 2004; accepted 1 May 2004
Available online 8 June 2004

Abstract

cis,trans-Fe(CO)$_2$(PMe$_3$)$_2$(*p*-Y-C$_6$H$_4$)X [X = Br, Y = H (**4a**), MeO (**4b**), Cl (**4c**), F (**4d**), Me (**4e**); X = I, Y = H (**5**); X = Cl, Y = H (**6**)] and *cis,trans*-Fe(CO)$_2$(PMe$_3$)$_2$(σ-CH=CH$_2$)X [X = Br (**7**); X = I (**8**); X = Cl (**9**)] are prepared by reacting dihalide complexes *cis,trans,cis*- Fe(CO)$_2$(PMe$_3$)$_2$X$_2$ [X = Br (**1**), X = I (**2**), X = Cl (**3**)] with Grignard reagents *p*-Y-C$_6$H$_4$-MgBr (Y = H, OMe, Cl, F, Me) or CH$_2$=CH–MgBr and with lithium reagents PhLi, CH$_2$=CH–Li. With both reagents, the reaction proceeds following two parallel pathways: one is the metallation reaction which yields alkyl derivatives, the other affords 17 electron complexes [Fe(CO)$_2$(PMe$_3$)$_2$X] via monoelectron reductive elimination. The influence of the halides and organometallic reagents on the yield of the metallation reaction is discussed. The solution structure of the complexes is assigned on the basis of IR and ^{1}H, ^{13}C, ^{19}F, ^{31}P NMR spectra. The solid state structure of complexes **4a**, **5** and **6** is determined by single crystal X-ray diffractometric methods.

Keywords: Syntheses; Phenyl complexes of iron; Vinyl complexes of iron; Halide iron complexes

1. Introduction

Alkyl and aryl complexes are very important in organometallic chemistry and in homogeneous catalysis because they are intermediates in the formation of C–C bonds [1]. They have been widely studied and various preparative methods have been used: nucleophilic attack on metal halides (organolithium or Grignard reagents), electrophilic attack on the metal (organic halide reagents), oxidative addition of organic halides and insertion of olefins in the M–H or M–C bond [2,3].

Comparing the methods reported in the literature to prepare the alkyl derivatives of the VIII group metals, almost all of the above-mentioned methods were used to prepare ruthenium monoalkyl Ru(CO)$_2$L$_2$RX (X = Cl, Br, I) and dialkyl Ru(CO)$_2$L$_2$RR′ (R,R′ = alkyl and aryl) complexes, as shown by Mawby and coworkers who used the transmetallation [4] and insertion [5] reactions and by our group that used the oxidative addition [6,7]. In contrast, only the oxidative addition of alkyl halides in tetracoordinated unsaturated d^8 intermediates [8] or pentacoordinated saturated d^8 compounds [9–11] was used to prepare the isoelectronic alkyl complexes of iron. In these last complexes, only the oxidative addition of the alkyl halides was effective, so it was not possible to prepare vinyl and aryl complexes.

In this work, we explore the possibility of using the metallation method with lithium and Grignard reagents to obtain the vinyl and aryl derivatives of iron.

2. Experimental

cis,trans,cis-Fe(CO)$_2$(PMe$_3$)$_2$X$_2$ (X = Br (**1**), I (**2**)) were prepared by reacting Fe(CO)$_4$X$_2$ [12] with PMe$_3$ in diethylether (DE), following the method described in [8a]. *cis,trans,cis*-Fe(CO)$_2$(PMe$_3$)$_2$Cl$_2$ (**3**) was prepared as described in [13]. Alkyl and aryl lithium, Grignard reagents Y-C$_6$H$_4$MgBr (Y = H, MeO, Cl, F, Me) and PMe$_3$ were commercial products. Vinyl lithium was prepared as described in [14]. Diethylether, tetrahydrofuran (THF) and dimethoxyethane (DME) were purified

---

* Corresponding author. Tel.: +39-075-5855578; fax:+39-075-5855 598.

E-mail address: cardchim@unipg.it (G. Cardaci).

0020-1693/$ - see front matter © 2004 Elsevier B.V. All rights reserved.
doi:10.1016/j.ica.2004.05.013

by refluxing with NaOH pellets, distilling, refluxing with Na and benzophenone and then freshly distilling under nitrogen before use; *n*-hexane was dehydrated with Na and distilled under nitrogen. All operations were carried out under nitrogen.

The ^{1}H, ^{31}P{^{1}H}, ^{19}F{^{1}H} and ^{13}C{^{1}H} NMR spectra were measured on a Bruker DRX 400 spectrometer; referencing was relative to TMS (^{1}H and ^{13}C), CCl_3F (^{19}F) and 85% H_3PO_4 (^{31}P). NMR samples were prepared by dissolving about 20 mg of the compounds in 0.5 ml of deuterated solvents. Infrared spectra were recorded on a Perkin–Elmer 1725X FTIR spectrophotometer. Elemental analyses were performed on a Carlo Erba 1106 elemental microanalyzer.

2.1. Reactions with Grignard reagents

*2.1.1. Preparation of cis,trans-Fe(CO)$_2$(PMe$_3$)$_2$(C$_6$H$_5$) Br (**4a**)*

The 0.5 g of complex **1** was dissolved in DE (30 ml); 1.1 ml of C_6H_5MgBr 3 M in DE (molar ratio 2/1) was added drop by drop to the stirred solution at room temperature. The colour of the solution changed instantaneously from red to green. The solution reacts with air, changing the colour from green to red, and $Fe(CO)_3(PMe_3)_2$ precipitated as yellow crystals ($\nu_{CO} = 1873$ cm^{-1} in DE). The supernatant solution was shaken with water and the ether phase separated and dried with $MgSO_4$. Complex **4a** was crystallized as orange crystals by *n*-hexane (yield 50%). *Anal.* Calc. for $C_{14}H_{23}BrFeO_2P_2$: C, 39.54; H, 5.51. Found: C, 39.32; H, 5.60%. ν_{CO}(cm^{-1}, DE): 2009, 1941.

^{1}H NMR (CD_2Cl_2): $\delta = 8.20$ (br, *o*-H), 7.59 (br, *o*-H), 7.06 (t, $^3J_{HH} = 7.00$, *m*-H), 6.98 (t, $^3J_{HH} = 6.6$, *p*-H), 1.37 (t_{Harris}, $^2J_{HP} + ^4J_{HP} = 8.6$, PMe$_3$). ^{13}C{^{1}H} NMR: $\delta = 217.7$ (t, $^2J_{CP} = 27.6$, CO *trans* Br), 209.4 (t, $^2J_{CP} = 14.3$, CO *trans* phenyl), 159.4 (t, $^2J_{CP} = 30.5$; C–Fe), 141.6 (s, *o*-C), 127.4 (s, *m*-C), 123.1 (s, *p*-C), 16.6 (t, $^1J_{CP} + ^3J_{CP} = 15.7$, PMe$_3$). ^{31}P{^{1}H} NMR: $\delta = 11.7$ (s, PMe$_3$).

*2.1.2. Preparation of cis,trans-Fe(CO)$_2$(PMe$_3$)$_2$(p-MeO-C$_6$H$_4$)Br (**4b**)*

Complex **4b** was prepared by reacting complex **1** and *p*-MeO-C_6H_4MgBr (1 M solution in THF) following the method described for complex **4a**. Yield: 41%. *Anal.* Calc. for $C_{15}H_{25}BrFeO_2P_2$: C, 39.94, H, 5.59. Found: C, 40.01; H, 5.51%. ν_{CO}(cm^{-1}, DE): 2008, 1941.

^{1}H NMR (CD_2Cl_2): $\delta = 8.00$ (br, *o*-H), 7.40 (br, *o*-H), 6.72 (d, $^3J_{HH} = 8.2$; *m*-H), 3.70 (s, OMe),1.36 (t_{Harris}, $^2J_{HP} + ^4J_{HP} = 8.4$, PMe$_3$). ^{13}C{^{1}H} NMR $\delta = 217.8$ (t, $^2J_{CP} = 27.3$, CO *trans* Br), 209.4 (t, $^2J_{CP} = 14.5$, CO *trans* phenyl), 157.3 (s, *p*-C), 146.2 (t, $^2J_{CP} = 33.0$, C–Fe), 141.4 (s, *o*-C), 114.0 (s, *m*-C), 55.2 (s, OMe),16.6 (t, $^1J_{CP} + ^3J_{CP} = 15.5$, PMe$_3$). ^{31}P{^{1}H} NMR: $\delta = 11.7$ (s, PMe$_3$).

*2.1.3. Preparation of cis,trans-Fe(CO)$_2$(PMe$_3$)$_2$(p-Cl-C$_6$H$_4$)Br (**4c**)*

Complex **4c** was prepared by reacting complex **1** and *p-Cl*-C_6H_4MgBr (1 M solution in DE) following the method described for complex **4a**. Yield: 40%. *Anal.* Calc. for $C_{14}H_{22}BrClFeO_2P_2$: C, 36.92 H, 4.87. Found: C, 36.75; H, 4.95%. ν_{CO}(cm^{-1}, DE): 2012, 1944.

^{1}H NMR (CD_2Cl_2): $\delta = 8.15$ (br, *o*-H), 7.50 (br, *o*-H), 7.06 (d, $^3J_{HH} = 7.9$, *m*-H), 1.37 (t_{Harris}, $^2J_{HP} + ^4J_{HP} = 8.6$, PMe$_3$). ^{13}C{^{1}H} NMR $\delta = 217.5$ (t, $^2J_{CP} = 26.7$, CO *trans* Br), 209.3 (t, $^2J_{CP} = 14.8$, CO *trans* phenyl), 158.2 (t, $^2J_{CP} = 30.9$, C–Fe), 143.2 (s, *o*-C), 142.2 (s, *o*-C), 129.9 (s, *p*-C), 127.1 (s, *m*-C), 16.5 (t, $^1J_{CP} + ^3J_{CP} = 15.8$, PMe$_3$). ^{31}P{^{1}H} NMR: $\delta = 11.3$ (s, PMe$_3$).

*2.1.4. Preparation of cis,trans-Fe(CO)$_2$(PMe$_3$)$_2$(p-F-C$_6$H$_4$)Br (**4d**)*

Complex **4d** was prepared by reacting complex **1** with *p*-F-C_6H_4MgBr (2 M solution in DE). Yield: 30%. *Anal.* Calc. for $C_{14}H_{22}BrFFeO_2P_2$: C, 38.30; H, 5.05. Found: C, 38.50; H, 4.96%. ν_{CO}(cm^{-1}, DE): 2013, 1944.

^{1}H NMR (CD_2Cl_2): $\delta = 8.15$ (br, *o*-H), 7.47 (br, *o*-H), 6.84 (dd, $^3J_{HH} = ^3J_{HF} = 8.0$, *m*-H), 1.36 ($t_{Harris}$, $^2J_{HP} + ^4J_{HP} = 8.2$, PMe$_3$). ^{13}C{^{1}H} NMR: $\delta = 217.6$ (t, $^2J_{CP} = 26.6$, CO *trans* Br), 209.4 (t, $^2J_{CP} = 14.8$, CO *trans* phenyl), 160.0 (d, $^1J_{CF} = 240.1$, C–F), 156.2 (t, $^2J_{CP} = 31.2$, C–Fe), 141.6 (s, *o*-C), 141.4 (s, *o*-C), 114.2 (s, *m*-C), 16.5 (t, $^1J_{CP} + ^3J_{CP} = 15.8$, PMe$_3$). ^{31}P{^{1}H} NMR: $\delta = 11.7$ (s, PMe$_3$). ^{19}F{^{1}H} NMR: $\delta = -124.8$ (m, *p*-F).

*2.1.5. Preparation of cis,trans-Fe(CO)$_2$(PMe$_3$)$_2$(p-Me-C$_6$H$_4$)Br (**4e**)*

Complex **4e** was prepared by reacting complex **1** with *p*-Me-C_6H_4MgBr (1 M solution in DE). Yield: 25%. *Anal.* Calc. for $C_{15}H_{25}BrFeO_2P_2$: C, 41.41; H, 5.79. Found: C, 41.60; H, 5.90%. ν_{CO}(cm^{-1}, DE): 2008, 1940.

^{1}H NMR (CD_2Cl_2): $\delta = 8.00$ (br, *o*-H), 7.40 (br, *o*-H), 6.90 (d, $^3J_{HH} = 7.8$, *m*-H), 2.3 (s, Me),1.37 (t_{Harris}, $^2J_{HP} + ^4J_{HP} = 8.2$, PMe$_3$). ^{13}C{^{1}H} NMR: 217.8 (t, $^2J_{CP} = 27.0$, CO *trans* Br), 209.3 (t, $^2J_{CP} = 14.3$, CO *trans* phenyl), 154.0 (t, $^2J_{CP} = 29.4$, C–Fe), 141.4 (s, *o*-C), 132.3 (s, *p*-C), 128.5 (s, *m*-C), 20.7 (s, Me), 16.6 (t, $^1J_{CP} + ^3J_{CP} = 15.4$, PMe$_3$). ^{31}P{^{1}H} NMR: $\delta = 11.6$ (s, PMe$_3$).

*2.1.6. Preparation of cis,trans-Fe(CO)$_2$(PMe$_3$)$_2$(m-Cl-C$_6$H$_4$)Br (**4f**)*

Complex **4f** was prepared by reacting complex **1** with *m*-Cl-C_6H_4MgBr (0.5 M solution in THF). Yield: 32%. *Anal.* Calc. for $C_{14}H_{22}BrClFeO_2P_2$: C, 36.3; H, 4.80. Found: C, 36.92; H, 4.87%. ν_{CO}(cm^{-1}, DE): 2012, 1946.

*2.1.7. Preparation of cis,trans-Fe(CO)$_2$(PMe$_3$)$_2$ (C$_a$H$_c$ = C$_b$H$_a$H$_b$)Br (**7**) (H$_a$ trans to H$_c$)*

Complex **7** was prepared by reacting complex **1** with ($CH_2{=}CH$)MgBr (1 M solution in THF) (molar ratio 1/

1) following the method described for the previous complexes. Yield: 56%. *Anal.* Calc. for $C_{10}H_{21}BrFeO_2P_2$: C, 32.38; H, 5.71. Found: C, 32.95; H, 5.83%. ν_{CO}(cm^{-1}, DE):2010, 1947.

^{1}H NMR (CD_2Cl_2): $\delta = 7.65$ (ddt, $^3J_{HcP} = 3.9$; $^3J_{HcHb} = 10.3$; $^3J_{HcHa} = 18.6$, H_c), 5.96 (ddt, $^4J_{HbP} = 6.2$; $^3J_{HbHc} = 10.3$; $^2J_{HbHa} = 1.8$, H_b), 5.96 (ddt, $^4J_{HaP} = 4.5$; $^3J_{HaHc} = 18.6$; $^2J_{HaHb} = 1.8$, H_a), $\delta = 1.53$ (t_{Harris}, $^2J_{HP} + {}^4J_{HP} = 8.3$, PMe_3). $^{13}C\{^1H\}$ NMR: 217.5 (t, $^2J_{CP} = 27.3$, CO *trans* Br), 208.9 (t, $^2J_{CP} = 14.1$, CO *trans* vinyl), 170 (t, $^2J_{CP} = 30.1$, C_a), 123.9 (s, C_b), 16.11 (t, $^1J_{CP} + {}^3J_{CP} = 15.6$, PMe_3). $^{31}P\{^1H\}$ NMR: $\delta = 12.0$ (s, PMe_3).

2.1.8. Reaction of complex 1 with (o-Me-C_6H_4)MgBr

Complex **1** reacted with (*o*-Me-C_6H_4)MgBr giving decomposition products.

2.1.9. Reaction of complex 1 with RMgX (R = Me, X = I; R = C_2H_5, X = Br)

Complex **1** reacts with alkyl Grignard reagents giving decomposition products.

2.2. Reaction with lithium reagents

2.2.1. Preparation of complex 4a

The 1 g of complex **1** was dissolved in DE (100 ml); PhLi (1.9 M solution in cyclohexane–ether mixture 70:30) was added drop by drop. The colour changed immediately from orange to green after reaction with air as observed for the Grignard reagents. The solution was shaken with H_2O to decompose the excess PhLi. The ether phase was separated and dried with $MgSO_4$; the solvent was evaporated and the residue was dissolved in *n*-hexane: complex **4a** was crystallized by this solvent as orange crystals: yield 90%.

The preparation of complex **4a** was carried out using the same procedure in *n*-hexane and THF. The yield varied greatly in function of the nature of the solvent: *n*-hexane, 18%; THF, 95%.

2.2.2. Preparation of cis,trans-$Fe(CO)_2(PMe_3)_2(C_6H_5)I$ (5)

The 0.5 g of complex **2** was dissolved in DE (30 ml); PhLi was added following the procedure described for the reaction with complex **1**. The reaction was immediate. Excess reagent was eliminated by shaking with H_2O. After separation of the ether phase, complex **5** was crystallized by *n*-hexane as red crystals: yield 80%. *Anal.* Calc. for $C_{14}H_{23}FeIO_2P_2$: C, 35.93; H, 4.95. Found: C, 36.02; H, 5.01%. ν_{CO}(cm^{-1}, DE): 2003, 1939.

^{1}H NMR (CD_2Cl_2): $\delta = 8.38$ (br, *o*-H), 7.64 (br, *o*-H), 7.00 (m, *m*-H e*p*-H), 1.47 (t_{Harris}, $^2J_{HP} + {}^4J_{HP} = 8.3$, PMe_3). $^{13}C\{^1H\}$ NMR: $\delta = 219.1$ (t, $^2J_{CP} = 26.4$, CO *trans* Br), 209.8 (t, $^2J_{CP} = 14.4$, CO *trans* phenyl), 157.8 (t, $^2J_{CP} = 31.3$, C–Fe), 146.5 (s, *o*-C), 141.6 (s, *o*-C), 127.7 (s, *m*-C), 123.0 (s, *p*-C), 18.1 (t, $^1J_{CP} + {}^3J_{CP} = 16.1$, PMe_3). $^{31}P\{^1H\}$ NMR: $\delta = 8.3$ (s, PMe_3).

2.2.3. Reaction of cis,trans-$Fe(CO)_2(PMe_3)_2Cl_2$ (3) with PhLi

The 0.5 g of complex **3** was dissolved at room temperature in DE (30 ml); 0.15 ml of PhLi (2 M solution in cyclohexane–ether mixture 70:30) was added drop by drop. The reaction was immediate and the red solution changed to green. The IR spectrum shows the formation of a complex with CO stretching bands at 1984 and 1935 cm^{-1}. Attempts to crystallize this complex were unfruitful owing to decomposition.

2.2.4. Preparation of cis,trans-$Fe(CO)_2(PMe_3)_2(C_6H_5)Cl$ (6)

The 0.1 g of complex **4a** was dissolved at room temperature in 15 ml of CH_2Cl_2, an excess of $(n\text{-}Bu)_4NCl$ (0.13 g) (molar ratio 1/50) was added and the solution was stirred for 1 h. The solution was dried and the residue was dissolved in *n*-hexane. Complex **6** was crystallized by the *n*-hexane solution at −20 °C as orange crystals. *Anal.* Calc. for $C_{14}H_{23}ClFeO_2P_2$: C, 44.65; H, 6.16. Found: C, 44.30; H, 6.28%. ν_{CO}(cm^{-1}, CH_2Cl_2): 2012, 1943.

^{1}H NMR (CD_2Cl_2): $\delta = 8.03$ (br, *o*-H), 7.56 (br, *o*-H), 7.08 (t, $^3J_{HH} = 7.0$, *m*-H), 6.99 (t, $^3J_{HH} = 6.9$; *p*-H), 1.31 (t_{Harris}, $^2J_{HP} + {}^4J_{HP} = 8.6$, PMe_3). $^{13}C\{^1H\}$ NMR: $\delta = 216.2$ (t, $^2J_{CP} = 26.8$, CO *trans* Br), 209.5 (t, $^2J_{CP} = 14.4$, CO *trans* phenyl), 161.3 (t, $^2J_{CP} = 30.4$, C–Fe), 141.5 (s, *o*-C), 139.2 (s, *o*-C), 127.3 (s, *m*-C), 123.2 (s, *p*-C), 15.8 (t, $^1J_{CP} + {}^3J_{CP} = 15.3$, PMe_3). $^{31}P\{^1H\}$ NMR: $\delta = 15.0$ (s, PMe_3).

2.2.5. Preparation of complex 7

The 100 mg of complex **1** ($2.38 \cdot 10^{-4}$ mol) was dissolved in DE (25 ml) at 0 °C. An equimolar quantity of $CH_2{=}CHLi$ in DE was added drop by drop to the stirred solution of complex **1**. The reaction was complete in 10 min. The solution was washed with water to decompose the excess of $CH_2{=}CHLi$; the ether phase was dehydrated by $MgSO_4$, then dried and complex **7** was crystallized as orange crystals by *n*-hexane at −20 °C. Yield: 95%.

2.2.6. Reaction of complex 2 with $CH_2{=}CHLi$

Complex **2** reacts with $CH_2{=}CHLi$ at room temperature. The formation of *cis*,*trans*-$Fe(CO)_2(PMe_3)_2(CH{=}CH_2)I$ (**8**) was observed by IR (ν_{CO}(cm^{-1}, DE): 2005, 1946). Complex **8** decomposed during the reaction with the formation of $Fe(CO)_3(PMe_3)_2$.

2.2.7. Preparation of complex cis,trans-$Fe(CO)_2(PMe_3)_2(C_aH_c{=}C_bH_aH_b)Cl$($H_a$ trans to H_c) (9)

The 100 mg of complex **3** (2.98×10^{-4} mol) was dissolved in DE (30 ml) at 0 °C. An equimolar quantity of $CH_2{=}CHLi$ was added drop by drop to the stirred solution of complex **3**. The reaction was instantaneous and the IR spectrum showed CO stretching bands at 2010 and 1945 cm^{-1}. The solution was washed with H_2O, the ether phase was dehydrated by $MgSO_4$ and dried. Complex **9** was crystallized by *n*-hexane as yellow crystals at −20 °C. Yield: 90%.

^1H NMR (CD_2Cl_2): $\delta = 7.44$ (ddt, $^3J_{HcP} = 3.8$; $^3J_{HcHb} = 10.4$; $^3J_{HcHa} = 18.7$, H_c), 5.95 (ddt, $^4J_{HbP} = 6.2$; $^3J_{HbHc} = 10.3$; $^2J_{HbHa} = 1.8$, H_b), 5.37 (ddt, $^4J_{HaP} = 4.0$; $^3J_{HaHc} = 18.7$; $^2J_{HaHb} = 1.8$, H_a), $\delta = 1.48$ (t $_{Harris}$, $^2J_{HP} + {}^4J_{HP} = 8.6$, PMe_3). $^{13}C\{^1H\}$ NMR: 216.6 (t, $^2J_{CP} = 27.0$, CO *trans* Br), 209.0 (t, $^2J_{CP} = 14.1$, CO *trans* vinyl), 172.7 (t, $^2J_{CP} = 30.0$, C_a), 123.5 (t, $^3J_{CP} = 5.8$, C_b), 15.3 (t, $^1J_{CP} + {}^3J_{CP} = 16.4$, PMe_3). $^{31}P\{^1H\}$ NMR: $\delta = 15.0$ (s, PMe_3).

2.2.8. Reaction with methyl lithium: preparation of *cis,trans,cis*-$Fe(CO)_2(PMe_3)_2(CH_3)_2$

The 1 g of complex **1** was dissolved in DE (100 ml); MeLi (1.6 M solution in DE) was added drop by drop. The reaction was monitored by IR. An immediate colour change from orange to red was observed. The IR controls showed that the reaction occurred in two steps: the first gave *cis,trans*-$Fe(CO)_2(PMe_3)_2MeBr$ ($\nu_{CO} =$ 1999, 1938 cm^{-1}), the second gave the dimethyl complex *cis,trans,cis*- $Fe(CO)_2(PMe_3)_2Me_2$ ($\nu_{CO} = 1973$, 1928 cm^{-1}). The solution was shaken with H_2O; the ether solution was evaporated and the dimethyl complex was crystallized by *n*-hexane: yield 86%. The NMR bands correspond to those of *cis,trans,cis*-$Fe(CO)_2(PMe_3)_2Me_2$ previously characterized by us [15]. The reaction was also carried out in DME, THF and *n*-hexane and the yield of the dimethyl complex was strongly dependent on the nature of the solvent: *n*-hexane, 29%; DME, 83%; THF, 95%.

2.3. X-ray crystallography

Monocrystals of complex **4a**, **5** and **6** were obtained by crystallization in *n*-hexane at −20 °C. Crystal data and details of structure refinement for complexes **4a**, **5** and **6** are reported in Table 1. Diffraction intensities were collected at 293 K on a XCALIBUR (Kuma 4CCD) diffractometer, using graphite monochromated Mo Kα ($\lambda = 0.70930$ Å). The scans and the frame data were acquired with CRYSALIS (CCD169) software. The crystal to detector distance was 65.77 mm. The frames were processed using CRYSALIS (RED 169) software to give the *hkl* file corrected for scan speed, background and Lorentz and polarization effects. Standard reflections, measured periodically, showed no apparent variation in intensity during data collection, so no correction for crystal decomposition was necessary. The data were corrected for absorption by using the SADABS [16] program. The structure was solved by direct methods using the SIR97 [17] program and refined on F^2 by the full-matrix least squares method using SHELXL-97 [18] WINGX [19] version. All non-hydrogen

Table 1
Crystal data and details for complexes **4a**, **5** and **6**

	Complex **4a**	Complex **5**	Complex **6**
Crystal habit	irregular prism	irregular prism	irregular prism
Crystal colour	orange	red	orange
Formula weight	421.02	468.01	376.56
Crystal system	monoclinic	monoclinic	monoclinic
Space group	$P2_1/c$	$P2_1/c$	$P2_1/c$
Cell parameters			
a (Å)	9.759(2)	9.818(10)	9.763(2)
b (Å)	15.252(2)	15.215(2)	15.354(2)
c (Å)	12.442(2)	12.663(2)	12.203(2)
β (°)	92.09(5)	91,31(1)	92.86(1)
V (Å^3)	1850.7(13)	1891.1(4)	1827.0(5)
Z	4	4	4
D_{calc} ($Mg\,m^{-3}$)	1.511	1.644	1.369
Absorption coefficient (mm^{-1})	3.145	2.597	1.145
Total data collected	16016	5639	12399
Unique observed data	3376	2131	5103
Criterion for observed	$F_c > 4\sigma(F_o)$	$F_c > 4\sigma(F_o)$	$F_c > 4\sigma(F_o)$
Unique data in the refinement (NO)	2740	1504	3287
Number of refined parameters (NV)	185	185	184
Overdetermination ratio (NO/NV)	14.8	8.1	17.8
R	0.0490	0.0605	0.0522
R_w	0.1158	0.1675	0.0988
GOF	1.077	1.130	1.039
$F(000)$	856	928	784
θ Range for data collection (°)	3.39–26.36	5.17–29.94	5.16–31.02

atoms were refined anisotropically. The hydrogen atoms were added at the calculated positions and refined using a riding model. Refinement converged at a final $R = 0.040$, $R_w = 0.1158$ and GOF = 1.077 for complex **4a**; $R = 0.0605$, $R_w = 0.1675$ and GOF = 1.130 for complex **5** and $R = 0.0502$, $R_w = 0.0988$ and GOF = 1.039 for complex **6** ($R = \sum ||F_o| - |F_c|| / \sum |F_c|$):

$$R_w = \left\{ \frac{\sum \left[w\left(F_o^2 - F_c^2\right)^2 \right]}{\sum \left[w\left(F_o^2\right)^2 \right]} \right\}^{1/2};$$

$$\mathrm{GOF} = \left\{ \frac{\sum \left[w\left(F_o^2 - F_c^2\right)^2 \right]}{(\mathrm{NO} - \mathrm{NV})} \right\}^{1/2}$$

where NO is the number of observed reflections and NV is the total number of parameters refined.

3. Results

3.1. Reactions with Grignard reagents

The reactions of complexes **1**–**3** with Grignard reagents RMgBr ($R = CH_3$, C_2H_5) yield decomposition products via the formation of 17 electron species [$Fe(CO)_2(PMe_3)_2X$], previously characterized by Berke [20]. This radical species react with oxygen giving $Fe(CO)_3(PMe_3)_2$. In contrast, the reaction with vinyl-MgBr and *p*-X-C_6H_4-MgBr (X = H, F, Cl, Me, OMe, Cl) follows two parallel pathways: one giving the 17 electron species [20], while the other yields *cis,trans*-$Fe(CO)_2(PMe_3)_2RX$ complexes, which were isolated and characterized.

The first reaction pathways proceed via a reductive elimination mechanism which gives the 17 electron species, according to the following scheme [21]:

$$\mathrm{RMgX} + \mathrm{Fe(CO)_2(PMe_3)_2X_2} \rightarrow \mathrm{Fe(CO)_2(PMe_3)_2X} + \mathrm{R}^{\cdot} + \mathrm{MgX_2}$$

The fate of $R^{\cdot}$ species was not determined.

In the second pathway, the Grignard reagent acts as a carbanion:

$$\mathrm{RMgX} + \mathrm{Fe(CO)_2(PMe_3)_2X_2} \rightarrow \mathrm{Fe\ (CO)_2(PMe_3)_2RX} + \mathrm{MgX_2}$$

m-C_6H_4-MgBr Grignard reagent reacts similarly to the *para* reagent, while the *ortho* reagent yield decomposition products. The yield of the aryl and vinyl complexes with respect to the reactant complex was determined by the spectroscopic absorbance of the CO stretching bands and follows the order:

Vinyl(56%) > Ph (50%) > *p*-OMe-C_6H_4 (41%) ≈ *p*-Cl-C_6H_4(40%) > *p*-F-C_6H_4(30%) ≈ *m*-Cl-C_6H_4(32%) > *p*-Me-C_6H_4(25%) ≫ *o*-X-C_6H_4(0%) ≈ CH_3(0%) ≈ C_2H_5(0%).

3.2. Reactions with lithium reagents

The behaviour of the lithium reagents follows the same scheme as the Grignard reagents; again, the reaction of RLi with complexes **1**–**3** follows two reaction pathways: one gives 17 electrons species via the radical mechanism:

$$P\mathrm{RLi} + \mathrm{Fe(CO)_2(PMe_3)_2X_2} \rightarrow \mathrm{Fe(CO)_2(PMe_3)_2X} + \mathrm{LiX} + \mathrm{R}^{\cdot}$$

The second pathway yields the alkyl derivatives according to the following scheme:

$$\mathrm{RLi} + \mathrm{Fe(CO)_2}(PMe_3)_2\mathrm{X_2} \rightarrow \mathrm{Fe(CO)_2(PMe_3)_2RX} + \mathrm{LiX}$$

The reaction with MeLi proceeds up to the formation of *cis,trans,cis*- $Fe(CO)_2(PMe_3)_2Me_2$ and it is not possible to isolate the mono alkyl derivative. Other alkyl lithium reagents (n-butyl, isopropyl, n-hexyl) react as MeLi, but the reaction products are unstable and decomposed during the purification. Vinyl lithium reacts at 0 °C with complex **1** in 10 min and with complex **3** instantaneously; on the contrary, the reaction with complex **2** occurs slowly at room temperature. Phenyl lithium reacts fast with $Fe(CO)_2(PMe_3)_2X_2$ (X = Br, I) giving complexes **4a** and **5**; on the contrary the reaction with the chloride derivative gives a very reactive paramagnetic complex, which was tentatively assigned to the 17 electron complex [$Fe(CO)_2(PMe_3)_2Cl$], similar to the complexes characterized by Berke [20]; then complex **6** was prepared by exchange of bromide with chloride in complex **4a**.

The yield of the metallation reaction in DE follows the order:

Vinyl(95%) > Ph(90%) > Me(80%).

The reaction between methyl lithium and complex **1** was carried out in various solvents: DE, DME, THF and *n*-hexane. The yield of the reaction increased with the polarity of the solvent following the order:

THF(95%) > DME(83%) ~ DE(86%) > *n*-hexane(29%).

3.3. Characterization in solution of *cis,trans*-$Fe(CO)_2(PMe_3)_2RX$

Cis,trans-$Fe(CO)_2(PMe_3)_2RX$ complexes (**4a**–**4e**, **5**–**9**) were characterized in solution by infrared spectroscopy and by ^1H, ^{13}C, ^{19}F and ^{31}P NMR spectroscopies. All *cis,trans*-$Fe(CO)_2(PMe_3)_2RX$ complexes show two CO stretching bands of equal intensity in IR, in agreement with the *cis*-position of the two CO ligands. The nature of R does not significantly influence the CO stretching frequencies. The CO stretching frequencies increased with the halides according to the trend Cl > Br > I, as observed in the isoelectronic series *cis,trans,cis*-$Fe(CO)_2(PMe_3)_2X_2$ and *cis,trans*-$Fe(CO)_2(PMe_3)_2CH_3X$.

The proton and carbon resonances of the phenyl group were assigned by using ^{1}H-COSY, ^{1}H, ^{13}C-HMQC and ^{1}H, ^{13}C-HMBC spectra. The ^{1}H and ^{13}C NMR spectra show a Harris triplet [22] assigned to the two PMe_3 ligands, indicating an octahedral structure with two PMe_3 in the *trans*-position.

All the phenyl complexes showed hindered rotation of the phenyl around the Fe–C bond. In fact at room temperature, complexes **4a**–**4d**, **5** and **6** showed two broad bands in the range 7–8.7 ppm, which were assigned to the *ortho* protons of the phenyl group. At 247 K, the *ortho* proton signals of complex **4a** became more structured, but maintained some fluxional character. The substituted phenyl derivatives **4c** and **4d** and the unsubstituted complexes **5** and **6** showed two *o*-C signals in the ^{13}C NMR spectra.

The $^{31}P\{^1H\}$ NMRspectra of all the complexes showed a singlet, confirming the *trans* structure of the PMe_3 ligands.

The chemical shifts of all the complexes were influenced by the halide and phenyl substituents. Selected NMR chemical shift data of the complexes synthesized in this work and of other isoelectronic halide complexes are given in Table 2. The chemical shifts of phosphorus and Fe–C carbon follow the trend $Cl > Br > I$, while those of the CO carbon *trans* to halide follow the inverse trend $I > Br > Cl$; the chemical shift of the CO *cis* to halide was hardly influenced. The trend observed for phosphorus was also observed in the series *cis*,*trans*,*cis*- $Fe(CO)_2(PMe_3)_2X_2$ and *cis*,*trans*-$Fe(CO)_2(PMe_3)_2$ CH_3X. This suggests that halides deshield iron following the trend $Cl > Br > I$ in agreement with the electronegativity of halide; so, the electron density on the iron increases as the atomic number of the halide increases. This observation is contrary to that reported by Tilset et al. for Cp*Fe(dppe)X complexes [X = F, Cl, Br, I; dppe = diphenylphosphineethane; Cp* = C_5Me_5] [23], but is the same of that reported by Gladysz et al. for the $CpRe(PPh_3)(NO)X$ series [24]. The inverse trend observed for the ^{13}C shift of the CO *trans* to halide suggests that, in this case, the dative π bonding effect, which follows the order $Cl > Br > I$ [25], can be important.

The halides influence the chemical shifts of the PMe_3 protons: $Cl(1,31) < Br(1.37) < I(1.47)$ and of the PMe_3 carbons: $Cl(15.8) < Br(16.6) < I(18.1)$; the reason for this behaviour is not clear.

The effect of the substituents in the phenyl group on the proton and carbon shifts of the ring in the complexes *cis*,*trans*-$Fe(CO)_2(PMe_3)_2$(*p*-X-C_6H_4)Br will be discussed assuming that the *para* position is that of X substituent; the *ortho* and *meta* positions of the ring are so defined, while the carbon bonded to the organometallic moiety will be indicated as C–Fe.

The effect of the X substituents on the proton chemical shifts cannot be evaluated for the *ortho* positions due to the fluxional behaviour of the protons. The effect of the substituents on the chemical shifts of the *meta* protons is very small. This could be due to the contrasting effect of the *para* substituents and the organometallic moiety $Fe(CO)_2(PMe_3)_2Br$ [26].

The effects of the X substituents on the ^{13}C chemical shifts are stronger than the proton shifts. They are similar to those observed in *p*-X-C_6H_4-$COCH_3$, as indicated by the linear trend of the chemical shift of *cis*,*trans*-$Fe(CO)_2(PMe_3)_2$(*p*- X-C_6H_4)Br with respect to the *para*-substituted benzoylacetones [27] reported in Fig. 1. The effect on the *para* carbon is the strongest. The effect of the substituents on the *meta* carbon shows the same trend as the *para* carbon, even if it is weaker. The effect of the substituents on the C–Fe group shows an inverted effect with respect to the *para* carbon; this effect is the same as that observed in benzoylacetone compounds and indicates that the $COCH_3$ and $Fe(CO)_2(PMe_3)_2Br$ groups exert the same withdrawing effect on the phenyl.

By comparing the ^{13}C chemical shifts of the iron complexes with the $Ru(CO)_2(PMe_2Ph)_2$(*p*-X-C_6H_4)$_2$ complexes [4b], a similar trend is observed with parallel effects on the different carbon atoms of the phenyl group.

Table 2
Selected NMR chemical shift data of isoelectronic alkylmonohalides and dihalides complexes of iron

Complexes	^{31}P NMR (ppm)	^{13}C NMR (ppm)		
		δ_{Fe-C}	δ_{CO}(*trans* to halide)	δ_{CO}(*trans* to alkyl)
cis,*trans*-$Fe(CO)_2(PMe_3)_2Br_2$ (**1**)	7.4			
cis,*trans*-$Fe(CO)_2(PMe_3)_2I_2$ (**2**)	−0.1			
cis,*trans*-$Fe(CO)_2(PMe_3)_2Cl_2$ (**3**)	13.6			
cis,*trans*-$Fe(CO)_2(PMe_3)_2C_6H_5Br$ (**4a**)	11.7	159.4	217.7	209.4
cis,*trans*-$Fe(CO)_2(PMe_3)_2C_6H_5I$ (**5**)	8.3	157.8	219.1	209.8
cis,*trans*-$Fe(CO)_2(PMe_3)_2C_6H_5Cl$ (**6**)	15.0	161.3	216.2	209.5
cis,*trans*-$Fe(CO)_2(PMe_3)_2(CH{=}CH2)Br$ (**7**)	12.0	170.0	219.1	209.8
cis,*trans*-$Fe(CO)_2(PMe_3)_2(CH{=}CH2)Cl$ (**9**)	15.0	172.7	216.6	209.0
cis,*trans*-$Fe(CO)_2(PMe_3)_2CH_3Br$	15.3			
cis,*trans*-$Fe(CO)_2(PMe_3)_2CH_3I$	11.4	−3.82	220.1	208.6
cis,*trans*-$Fe(CO)_2(PMe_3)_2CH_3Cl$	18.6			

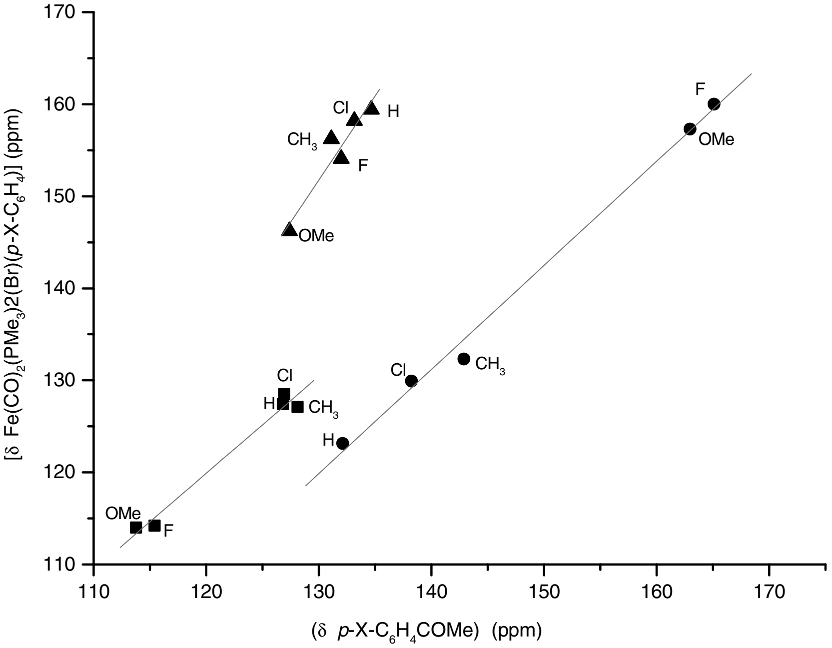

Fig. 1. ^{13}C chemical shifts of phenyl carbons in *cis,trans*-$Fe(CO)_2(PMe_3)_2Br$(*p*-X- C_6H_4) vs ^{13}C chemical shifts of phenyl carbons in *p*-X-C_6H_4-$COCH_3$: ● *para*-carbon; ▲ C-Fe; ■ *meta*-carbon.

The phenyl substituents do not appreciably influence the chemical shifts of the PMe_3 and CO ligands.

The NMR signals of complexes **7** and **9** were assigned on the basis of the vinyl proton couplings and by comparing the chemical shifts of the isoelectronic vinyl complexes of ruthenium [28,29].

As previously observed for isoelectronic complexes of iron and ruthenium, the coupling constants in the iron complexes were higher than those in the ruthenium complexes [30].

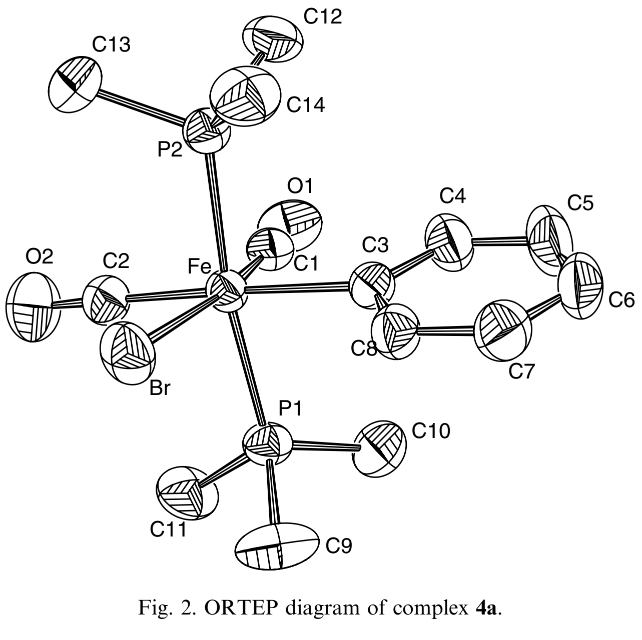

Fig. 2. ORTEP diagram of complex **4a**.

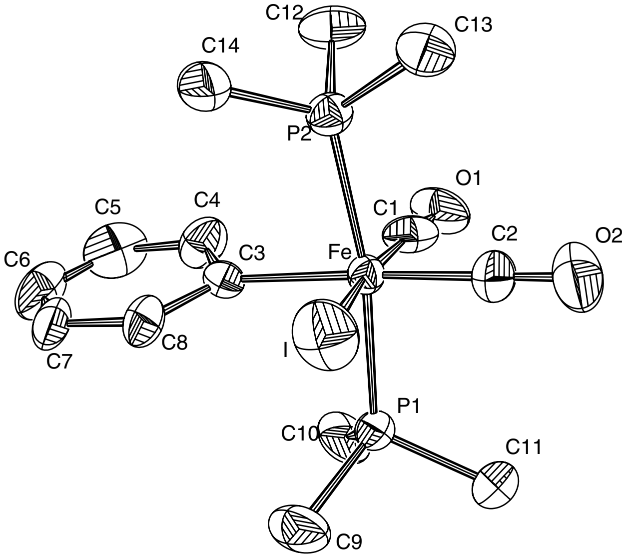

Fig. 3. ORTEP diagram of complex **5**.

3.4. Solid structures

The molecular structures of complexes **4a**, **5** and **6** in the solid state, obtained by single crystal X-ray diffraction methods, are given in Figs. 2–4, in which the same crystallographic numbering was used. Table 3 reports selected bond distances and angles for the three complexes. The three structures are very similar. The iron

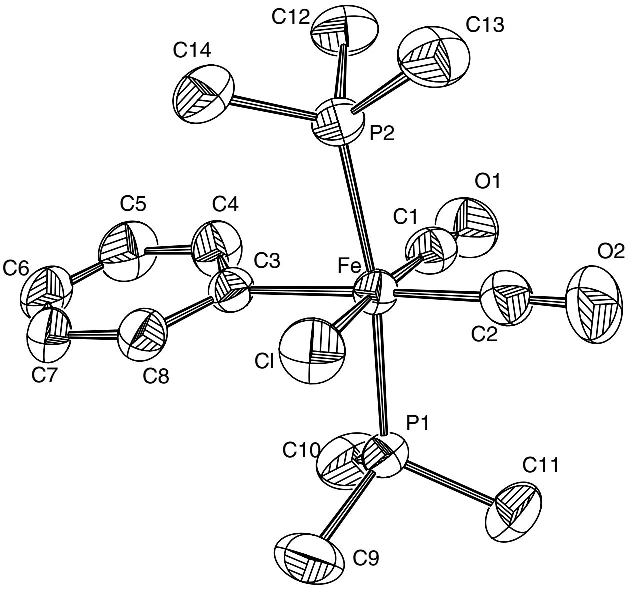

Fig. 4. ORTEP diagram of complex **6**.

atom exhibits the expected octahedral geometry with the trimethylphosphine ligands occupying the *trans* position and the other ligands occupying the four coordination positions in the perpendicular plane with the CO ligands in the *cis* position.

Besides Fe–Br, Fe–I and Fe–Cl, only Fe–C(3) is notably different in complexes **4a**, **5** and **6** (Fe–C(3) = 2.093 Å for **4a**, 2.058 Å for **5** and 2.057 Å for **6**). All the other distances and angles are very similar and will be discussed at the same time. The trimethylphosphine ligands are bent toward the phenyl substituent (P(2)–Fe–P(1) = 170.99° for **4a**, 170.81° for **5** and 171.06° for **6**). The C(3)-Fe-halide angles are more than 90° (96° for **4a**, 96.7° for **5** and 94.74° for **6**): this supports an interaction of the halides and the *meta* hydrogen of the phenyl group as confirmed by the torsion of the phenyl plane with respect to the mean equatorial plane of the octahedral structure ($\vartheta = 9.9°$ for **4a**, 8.7° for **5** and 10.6 for **6**) and by the contact distances between the protons and the halide atom (2.688 Å for **4a**, 2.785 Å for **5** and 2.587 Å for **6**). Contact distances can also be observed between the phosphine hydrogens and the halides (2.921 Å for **4a**, 3.004 Å for **5** and 2.8388 Å for **6**). The torsion angle increases in the series Cl>Br>I and can be explained on the basis of a balance of the halide radius and of the Fe-halide bond distance.

Table 3
Relevant bond lengths (Å) and angles (°) for complexes **4a**, **5** and **6**

	Complex **4a**	Complex **5**	Complex **6**
Fe–C(1)	1.767(6)	1.762(18)	1.758(3)
Fe–C(2)	1.800(5)	1.778(15)	1.796(3)
Fe–C(3)	2.093(4)	2.058(13)	2.057(3)
Fe–P(2)	2.2540(14)	2.251(4)	2.2534(9)
Fe–P(1)	2.2585(15)	2.260(4)	2.2587(9)
Fe–Hal	2.5128(12)	2.61(3)	2.3717(10)
O(1)–C(1)	1.047(6)	1.063(19)	1.088(4)
O(2)–C(2)	1.133(6)	1.151(18)	1.140(4)
C(1)–Fe–C(2)	90.2(2)	90.6(8)	90.73(13)
C(1)–Fe–C(3)	93.0(2)	92.7(7)	92.15(12)
C(2)–Fe–C(3)	176.6(2)	176.4(7)	176.99(11)
C(1)–Fe–P(2)	92.46(16)	92.2(5)	92.68(9)
C(2)–Fe–P(2)	95.56(17)	95.4(5)	95.35(9)
C(3)–Fe–P(2)	85.53(13)	86.1(4)	85.39(7)
C(1)–Fe–P(1)	89.34(16)	89.9(5)	88.87(9)
C(2)–Fe–P(1)	93.27(17)	93.5(5)	93.43(9)
C(3)–Fe–P(1)	85.56(13)	84.9(4)	85.75(7)
P(2)–Fe–P(1)	170.99(5)	170.83(16)	171.06(3)
C(1)–Fe–Hal	170.85(17)	170.4(10)	172.99(10)
C(2)–Fe–Hal	80.83(16)	80.0(9)	82.40(9)
C(3)–Fe–Hal	96.02(13)	96.7(9)	94.74(8)
P(2)–Fe–Hal	86.59(5)	86.7(5)	86.63(3)
P(1)–Fe–Hal	93.02(5)	92.7(5)	92.89(3)

4. Discussion

The values of ^{31}P and ^{13}C chemical shifts of the ligands in organometallic complexes are used in the literature [23] to obtain information about the electronic density on the iron atom: the greater the chemical shifts of ^{31}P and ^{13}C, the greater the electron density on the iron.

In Table 2 the chemical shifts of ^{31}P and, in some cases, of ^{13}C of the complexes *cis*,*trans*,*cis*-$Fe(CO)_2(PMe_3)_2X_2$, *cis*,*trans*-$Fe(CO)_2(PMe_3)_2$ $(C_6H_5)X$, *cis*,-*trans*-$Fe(CO)_2(PMe_3)_2(CH{=}CH_2)X$ and *cis*,*trans*-$Fe(CO)_2(PMe_3)_2(CH_3)X$ (X = Cl, Br, I) are given. On the basis of these chemical shifts, the electron density on the iron follows the trend I > Br > Cl in agreement with the σ-electron withdrawing power of the halides [25]. Studies of the halide exchange in the series *cis*,*trans*-$Fe(CO)_2(PMe_3)_2$ $(CH_3)X$ (X = Cl, Br, I) [31] and the halide exchange results obtained in this work indicate that the exchange equilibrium follows the trend Cl > Br > I; therefore, in the previous series the behaviour of the iron atom was hard.

So both the monoelectron radical reduction and the nucleophilic attack of carbanion with Grignard and lithium reagents should be easier with the decreasing electron density on the iron and the reaction rate should follow the trend Cl > Br > I, as observed for the reactions for which a difference in the reaction rates has been observed as in the reactions of *cis*,*trans*-$Fe(CO)_2(PMe_3)_2X_2$ (X = Cl, Br, I) with vinyl lithium.

The yield of the radical reaction with respect to the metallation reaction depends prevalently on the properties of the organometallic reagents: with the lithium reagents the metallation reaction is prevailing (yield ~80–95%), while with the Grignard reagents the radical reaction is prevailing (yield ~45–100%). This is in agreement with the general behaviour of the Grignard reagents, which show a greater disposition to radical reaction [21] than the lithium reagents.

The yield of the metallation reaction with both Grignard and lithium regents is higher with vinyl and phenyl than with alkyl derivatives. This behaviour can be explained on the basis of the higher stability of the vinyl and phenyl carbanions, which is measured by the PK_a of the corresponding hydrocarbons [32,33] or by the oxidation potential of Grignard [34] and lithium reagents [35].

Polar solvents increase the yield of the metallation reaction: this effect can also be explained by the solvatation of the carbanions, which increases their stability according to the Born model [36].

5. Supplementary material

Crystallographic data for the structural analysis have been deposited with the Cambridge Crystallographic Data Center, CCDC No. 225543 for complex **4a**, CCDC No. 225544 for complex **5** and CCDC No. 225545 for complex **6**. Copies of this information may be obtained free of charge from The Director, CCDC, 12 Union Road, Cambridge, CB2 1EZ, UK (fax: +44-1223-336033; e-mail: deposit@ccdc.cam.ac.uk or www.ccdc.cam.ac.uk).

Acknowledgements

The authors thank Dr. Cristiano Zuccaccia for useful discussion. This work was supported by grant from the Ministero dell'Istruzione, dell'Università e della Ricerca (MIUR, Rome, Italy), Programma di Rilevante Interesse Nazionale, Cofinanziamento 2002–2003.

References

[1] (a) J.M. Brown, N.A. Cooley, Chem. Rev. 88 (1988) 1031;
(b) J.K. Stille, in: F.R. Hartley, S. Patai (Eds.), The Chemistry of the Metal–Carbon Bond, Vol. 2, Wiley, New York, 1985;
(c) W.A. Hermann, Applied Homogeneous Catalysis with Organometallic Compounds, VCH Publishers, New York, 1988.
[2] R.H. Crabtree, The Organometallic Chemistry of the Transition Metals, Wiley, New York, 1988.
[3] J.P. Collman, C.S. Hegedus, J.R. Norton, R.G. Finke, Principles and Application of Organotransition Metal Chemistry, University Science Books, Mill Valley, CA, 1987.
[4] (a) C.F.J. Barnard, J.A. Daniels, J. Jeffery, R.J. Mawby, J. Chem. Soc., Dalton Trans. (1976) 953;
(b) D.R. Saunders, M. Stephenson, R.J. Mawby, J. Chem. Soc., Dalton Trans. (1983) 2473.
[5] M.P. Waugh, R.J. Mawby, A.J. Rent, R.J. Carter, C.A. Reynolds, Inorg. Chim. Acta 240 (1995) 263.
[6] G. Cardaci, J. Organometal. Chem. 323 (1987) C10.
[7] G. Bellachioma, G. Cardaci, A. Macchioni, A. Madami, Inorg. Chem. 32 (1993) 554.
[8] (a) G. Cardaci, G. Bellachioma, P.F. Zanazzi, Organometallics 7 (1988) 172;
(b) R. Birk, H. Berke, G. Huttner, L. Zsolnai, Chem. Ber. 121 (1988) 1557.
[9] M. Pankowski, M. Bigorgne, J. Organometal. Chem. 30 (1971) 227.
[10] G. Reichenbach, G. Cardaci, G. Bellachioma, J. Chem. Soc., Dalton Trans. (1982) 847.
[11] C.R. Jablonski, Inorg. Chem. 20 (1981) 3940.
[12] I.A. Cohen, F. Basolo, J. Inorg. Nucl. Chem. 28 (1966) 511.
[13] F. Mercier, F. Mathey, J. Augenault, J. Couturier, Y. Marey, J. Organometal. Chem. 231 (1982) 237.
[14] G. Frenkel, H. Hyer, B.W. Su, in: R.O. Bach (Ed.), Lithium: Current Applications in Sciece Technology and Medicine, Wiley-Interscience, New York, 1985, p. 273.
[15] G. Bellachioma, G. Cardaci, A. Macchioni, C. Zuccaccia, Organometal. Chem. 628 (2001) 255.
[16] G.M. Sheldrick, SADABS:Program for the empirical correction of area detector data, University of Gottingen, germany, 1996.
[17] A. Altomare, M.C. Burla, M. Camalli, G. Cascarano, C. Giacovazzo, A. Gagliardi, A.G.G. Moliterni, G. Polidori, R. Spagna, J. Appl. Cryst. 32 (1999) 115.
[18] G.M. Sheldrick, SHELXL-97, University of Gottingen, Germany, 1997.
[19] L.J. Farrugia, J. Appl. Cryst. 32 (1999) 837.
[20] H. Kandler, C. Gauss, W. Bidell, S. Rosenberger, T. Burgi, I.L. Eremenko, D. Veghini, O. Orama, P. Burger, H. Berke, Chem. Eur. J. 1 (1995) 541.
[21] W.E. Lindsell, in: G. Wilkinson (Ed.), Comprehensive Organometallic Chemistry, vol. 1, Pergamon Press, Oxford, 1982, pp. 181–187.
[22] R.K. Harris, Can. J. Chem. 39 (1961) 216.
[23] M. Tilset, I. Fjeldahl, J.-R. Hamon, P. Hamon, L. Toupet, J.-Y. Saillard, K. Costuas, A. Haynes, J. Am. Chem. Soc. 123 (2001) 9984.
[24] S.K. Agbossou, C. Roger, A. Igau, J.A. Gladysz, Inorg. Chem. 31 (1992) 419.
[25] K. Fagnon, M. Lautens, Angew. Chem., Int. Ed. 41 (2002) 26.
[26] A.R. Tarpley, H. Goldstein, J. Phys. Chem. (1972) 515.
[27] R.M. Cravero, M. Gonzalez-Sierra, A.C. Olivieri, J. Chem. Soc., Perkin Trans. II (1993) 1067.
[28] M. Bray, R.J. Mawby, J. Chem. Soc., Dalton Trans. (1989) 744.
[29] M.P. Waugh, R.J. Mawby, J. Chem. Soc., Dalton Trans. (1997) 21.
[30] M. Aubert, G. Bellachioma, G. Cardaci, A. Macchioni, G. Reichenbach, M.C. Burla, J. Chem. Soc., Dalton Trans. (1997) 1759.
[31] G. Reichenbach, G. Bellachioma, R. Cambi, G. Cardaci, C. Lanfaloni, A. Macchioni, R. Ricci, G. Vetralla, Inorg. Chim. Acta 288 (1999) 200.
[32] I. Kosuke, Acid-base Dissociation Constants in dipolar Aprotic Solvents, Chemical Data Series n.35, Blackwell Scientific Publications, Oxford, 1990.
[33] F.G. Bordwell, Acc. Chem. Res. 21 (1988) 456.
[34] G.A. Russell, D.W. Lanson, J. Organometal. Chem. 156 (1978) 17, and reference therein.
[35] B. Jaun, J. Schwarz, R. Breslow, J. Am. Chem. Soc. 102 (1980) 5741.
[36] K. Daasbjierg, Acta Chem. Scand. 49 (1995) 875.